Diamond growth in mantle fluids

Hélène Bureau, Daniel J. Frost, Nathalie Bolfan-Casanova, Clémence Leroy,
Imène Esteve, Patrick Cordier

1 # Diamond growth in mantle fluids

2

3 **Hélène Bureau[a*], Daniel J. Frost[b], Nathalie Bolfan-Casanova[c], Clémence Leroy[a], Imène**

4 **Esteve[a], Patrick Cordier[d]**

5

6

7 *[a] Institut de Minéralogie, de Physique des Matériaux et de Cosmochimie (IMPMC), Sorbonne*

8 *Universités – UPMC Univ. Paris 06, CNRS UMR 7590, Muséum National d'Histoire*

9 *Naturelle, IRD UR 206, 4 place Jussieu, 75252 Paris Cedex 05, France*

10 *[b] Bayerisches Geoinstitut, Universität Bayreuth, D-95440 Bayreuth, Germany*

11 *[c]Laboratoire Magmas et Volcans, Université Blaise Pascal, Clermont-Ferrand, France*

12 *[d] Unité Matériaux et Transformations, Université Lille 1, 59655 Villeneuve d'Ascq, France*

13

14

15

16

17

18 Revised manuscript for submission to Lithos: SI Diamonds

19

20

21

22 *Corresponding author.

23   *E-mail address: Helene.bureau@impmc.upmc.fr*, *Tel.* +33 1 44274807

24

26   **Abstract**

27   In the upper mantle, diamonds can potentially grow from various forms of media (solid,

28   gas, fluid) with a range of compositions (e.g. graphite, C-O-H fluids, silicate or carbonate

29   melts). Inclusions trapped in diamonds are one of the few diagnostic tools that can constrain

30   diamond growth conditions in the Earth's mantle. In this study, inclusion-bearing diamonds

31   have been synthesized to understand the growth conditions of natural diamonds in the upper

32   mantle. Diamonds containing syngenetic inclusions were synthesized in multi-anvil presses

33   employing starting mixtures of carbonates, and silicate compositions in the presence of pure

34   water and saline fluids (H_2O-NaCl). Experiments were performed at conditions compatible

35   with the Earth's geotherm (7 GPa, 1300-1400°C). Results show that within the timescale of the

36   experiments (6 to 30 hours) diamond growth occurs if water and carbonates are present in the

37   fluid phase. Water promotes faster diamond growth (up to 14 mm/year at 1400°C, 7 GPa, 10

38   g/l NaCl), which is favourable to the inclusion trapping process. At 7 GPa, temperature and

39   fluid composition are the main factors controlling diamond growth. In these experiments,

40   diamonds grew in the presence of two fluids: an aqueous fluid and a hydrous silicate melt. The

41   carbon source for diamond growth must be carbonate (CO_3^{2}) dissolved in the melt or carbon

42   dioxide species in the aqueous fluid (CO_{2aq}). The presence of NaCl affects the growth kinetics

43   but is not a prerequisite for inclusion-bearing diamond formation. The presence of small

44   discrete or isolated volumes of water-rich fluids is necessary to grow inclusion-bearing

45   peridotitic, eclogitic, fibrous, cloudy and coated diamonds, and may also be involved in the

46   growth of ultradeep, ultrahigh-pressure metamorphic diamonds.

47

48

49

50

1. Introduction

The growth mechanism of natural diamonds in the Earth's mantle is still an open and debated issue in Earth Sciences (e.g. Stachel and Harris, 2009; Harte, 2010; Shirey et al., 2013 and all references therein). Diamond is a metasomatic mineral that formed through redox reactions of mobile C-bearing phases (fluids/melts) that percolate in the mantle over a large range of depths suggesting different kind of carbon sources. The nature and storage modes for carbon at depth are still poorly understood. This is mostly because, unlike to hydrogen, carbon is not significantly incorporated into the major rock-forming minerals of the mantle but instead forms accessory phases. Depending on the depth these accessory phases may evolve from fluids/melts, carbonates, diamond, Fe-rich alloys, or metal carbide. For that reason diamond growth scenarios in the different mantle regions (upper, transition zone and lower) are still undefined. A systematic investigation of the phases trapped in natural diamonds as inclusions is of primary relevance to constrain diamond genesis as well as to understand carbon storage and cycling in the mantle.

Most natural diamonds are brought up to the Earth's surface through kimberlitic volcanism in ancient cratonic lithosphere, but monocrystalline and sublithospheric diamonds can also be found in alluvial deposits. Due mainly to differences in their inclusions, we distinguish diamonds formed in the lithosphere from those that are formed below the lithosphere in the convecting mantle. The majority of the gem quality monocrystalline diamonds are from the lithosphere. They have eclogitic or peridotitic (the most abundant) associations depending on the mineral assemblage of their inclusions, and come from depths of at least 200 km, based on the phase equilibria of their solid inclusions (Stachel and Harris, 2009; Harte, 2010). Recently, fluid inclusions of high-density saline fluids have been found in very

4

74 old monocrystalline diamonds (Weiss et al., 2014) possibly implying a morphological

75 continuum between monocrystalline diamonds and fibrous diamonds, another species of

76 lithospheric diamonds. The later are characterized by their high density of fluid and mineral

77 inclusions (Klein Ben David et al 2010 and references therein). The fluids reflect oxidizing

78 conditions and show a variety of compositions between carbonatitic, silicic and saline end-

79 members. These fluids are the crucial deciphering tools for diamond growth mechanisms as

80 they represent the "medium" in equilibrium during diamond growth (e.g. Navon et al., 1988

81 Klein BenDavid et al., 2010 and references therein). A final form in which diamonds are found

82 are as polycrystalline assemblages (Heaney et al. 2005) such as framesites (e.g. Kurat and

83 Dobosi, 2000) and carbonados (e.g. Sautter et al., 2011). Carbonados are exclusively found as

84 pebbles within placers and are not known to be associated with kimberlitic rocks, so their origin

85 is still a matter of debate. Moreover carbonados completely lack typical mantle-derived

86 inclusions and may contain assemblages of native minerals and metals (protogenetic inclusions

87 of augite and ilmenite - i.e. seeds for diamond nucleation), pointing to a genesis characterized

88 by highly reducing conditions (FMQ-15 log units, Sautter et al. 2011 and ref. therein). These

89 diamonds are characterized by tiny micrometer-sized crystals found in crustal rocks originally

90 subducted to ultrahigh pressures (e.g. De Corte, et al., 1998; Dobrzhinetskaya, 2012 for a

91 review).

92 Diamonds grow through metsomatic processes involving C-O-H bearing fluids or melts.

93 The nature of these fluids likely varies depending on the particular diamond forming conditions.

94 It has been proposed, for example, that unlike diamonds from the upper mantle that grow within

95 oxidized fluids, ultra-deep diamonds (i.e. from the lower mantle) derive from reduced fluids

96 (Stachel and Harris, 2009). The recent discovery of a OH-bearing ringwoodite inclusion in a

97 diamond from the transition zone (Pearson et al., 2014) implies that transition zone diamonds

98 may grow from hydrogen-bearing melts or fluids. Diamonds therefore allow carbon behavior

99   in the deep Earth to be traced but also provide crucial and unique information concerning the

100 deep cycling of other volatile species. Water and halogens, for example, are commonly found

101 as high density fluids (HDF) trapped as inclusions mainly in fibrous, coated and cloudy

102 diamonds (e.g. Navon et al., 1998; Johnson et al., 2000; Izraeli et al., 2001; Burgess et al., 2002;

103 Klein-BenDavid et al., 2007; Tomlinson et al., 2006; 2009; Weiss et al., 2009; Pearson et al.,

104 2014; Weiss et al., 2014). Furthermore, whereas most HDFs are found in fibrous and coated

105 diamonds, a recent report of HDF trapped in monocristalline diamonds from the Phanerozoic

106 carrying a peridotitic signature (Weiss et al., 2014) points to a role of HDF in the growth of

107 these diamond gems.

108   Indications concerning the parental "fluids" of diamonds and the locus of their growth

109 in the mantle can be obtained by studying the composition of natural inclusions trapped in

110 diamonds (Pearson et al., 2014; Novella et al., 2015), and from the isotopic carbon and nitrogen

111 signatures of diamonds (see the review after Cartigny 2014; Mikhail et al. 2014). The

112 association of diamond growth with subduction zones is frequently proposed because

113 subduction recycles hydrous and relatively oxidized fluids (Stachel et al., 2005). However, this

114 concept is highly debated, based on carbon and nitrogen isotope signatures of natural diamonds

115 (Cartigny et al., 2014). Indeed, most of the natural diamond gems, including fibrous and coated

116 diamonds, exhibit mantle-derived carbon $\delta^{13}C$ ranges from -10 to -5‰ whereas sedimentary

117 carbon, recycled at subduction zones, ranges from -45 to +4‰, with the range for organic matter

118 being -45 to -15‰ and -3 to 4‰ for carbonates (Cartigny et al., 2014). Some diamonds exhibit

119 a light signature with respect to carbon suggesting that the recycled carbon participates to the

120 growth of these diamonds (e.g. Kaminsky and Wirth, 2009, Walter et al., 2011, Mikhail et al.

121 2013; Thomson et al., 2014; Zedgenizov et al., 2014; Bulanova et al., 2014). This is supported

122 by the oxygen isotope composition of inclusions trapped in superdeep diamonds (Burnham et

123 al., 2015).

124 An alternative possibility is that the isotopic variability recorded in diamonds might also reflect

125 a fractionation process occurring during diamond formation (e.g. Cartigny et al., 2014). In

126 summary, diamond formation from C-O-H-N-S fluids (or melts) is quite likely but the source

127 and mechanism remain poorly understood (Stachel and Luth, 2015 and references therein).

128 One way to address these issues is through laboratory experiments. Diamond growth

129 experiments at pressures and temperatures relevant to the Earth's interior have been conducted

130 by numerous researchers over the last decades. Pal'Yanov et al. (1999) were among the first to

131 experimentally demonstrate the practicality of diamond-growth from a mixture of carbonates

132 and water. Since this study, additional experimental studies have shown that diamonds can grow

133 in complex fluid mixtures, including silicates and saline fluids (e.g. Arima et al., 1993;

134 Pal'yanov et al. 2007; Safonov et al., 2007; 2011; Sokol Pal'Yanov, 2008; Pal'Yanov et al.,

135 2007; Pal'Yanov and Sokol, 2009 and references therein; Arima et al., 2010; Fangan and Luth,

136 2010; Bureau et al., 2012).

137 Paradoxically, experimental diamond growth has been achieved using numerous fluid

138 mixtures, and this makes the identification of parental fluids of natural diamonds quite difficult.

139 One approach to more tightly constrain the parental fluids of natural diamonds is to reproduce

140 the inclusions found in diamonds during growth experiments. In a previous study Bureau et al.

141 (2012) were successful in growing diamond bearing inclusions from a mixture of silicate,

142 carbonates and water. Depending on experimental conditions (from 7 to 9 GPa, from 1200 to

143 1700°C), these inclusions comprised aqueous fluids, silicate glasses or minerals. It was shown

144 that water is a key parameter to grow diamond bearing inclusions in the upper mantle, and that

145 diamonds having trapped inclusions must have experienced fast growth rates. The study has

146 showed that depending on the pressure and temperature conditions, upper mantle diamonds are

147 possibly growing from one single supercritical fluid or from two fluids, aqueous fluid and

148 silicate melt, in equilibrium with each other. This preliminary study was performed with simple

149 starting compositions (pure water, iron-free system) and therefore the inclusions trapped in the

150 new experimentally grown diamonds were not representative in composition of the inclusions

151 observed in natural diamonds because, for example, iron was not present in the system.

152   In the present work, we have experimentally grown diamonds from fluids containing

153 significant amounts of water (pure and saline), together with silicates and carbonates (synthetic

154 and natural). Mineralogical assemblages similar to those found as inclusions in natural

155 diamonds are obtained as inclusions in experimentally grown diamonds.

156

157   **2. Materials and methods**

158 Synthetic and natural powders of various compositions were employed as starting materials, as

159 described in Table 1. We have used: (1) the same mixture MELD of synthetic powders already

160 used in a previous study (Bureau et al., 2012), which has the average composition of natural

161 inclusions trapped in fibrous diamonds, from the study of Navon et al. (1998), but is iron-free;

162 (2) SIDB a mixture of MELD mixed with 10 wt.% natural siderite ($FeCO_3$), in order to add

163 iron; and (3) SED, a mixture of 33.33 wt.% of natural pelagic sediment with 66.66 wt.% of a

164 natural Mid Ocean Ridge Basalt (MORB). These powders were loaded into Pt or AuPd capsules

165 together with pure graphite as a carbon source, and either pure water or solutions of H_2O-NaCl

166 (10 and 30 g/l). We used commercial diamond seeds (diameter: 20-30 µm or 40-60 µm)

167 oxidized in a HT furnace at 1000° for 10 minutes in order to modify the surface of the seeds to

168 form cavities that favor inclusion trapping. The capsules were carefully sealed by welding in

169   order to avoid any fluid loss. Each capsule contained 40 wt.% of one of the three powders, 40

170   wt.% of fluid, 10 wt.% graphite, and 10 wt.% diamond seeds.

171   Experiments were performed in multi-anvil devices at BGI, Bayreuth and at LMV, Clermont-

172   Ferrand. The high-pressure assembly comprised a 18 mm edge-length MgO octahedron,

173   together with tungsten carbide anvils of 11 mm edge length truncations. Graphite or $LaCrO_3$

174   heaters were used and temperatures were measured using W(3%Re)–W(25%Re)

175   thermocouples.

176   The experiments were performed at 6-7 GPa and from 1300°C to 1400°C, for run durations

177   between 6 and 30 hours. After each synthesis the experiment was quenched to room temperature

178   before slow decompression. Capsules were weighed before and after opening to check for the

179   presence of aqueous fluids. The remaining solid products were mounted on stubs covered with

180   carbon tape and studied by Scanning Electron Microscopy (SEM) with a Zeiss Crossbeam

181   Neon40 at IMPMC. The interiors of some diamond seeds were exposed using a Focus Ion Beam

182   (FIB). Galium beams were used either with a Zeiss Crossbeam Neon40 at IMPMC (Paris,

183   France) or a FEI Strata DB 235 at IEMN (Lille France). The FIB sections were deposited on

184   silicon wafers for planar investigations. Quantitative chemical analyses were obtained by the

185   energy dispersive X-ray (EDX) technique in conjunction with either an SEM or FIB. The

186   detector was calibrated with a pure copper target at the start of the session to determine the

187   beam current. EDS semi-quantitative analyses were performed and calibrated using

188   international standards employed for electron microprobe analysis in order to perform spectra

189   deconvolution and quantitification. Moreover the quantification was validated using a range of

190   further well characterized standards: a panteleritic galss (KE12, Métrich and Rutherford, 1992),

191   a basaltic glass from Piton de la Fournaise volcano (Bureau et al., 1998), a synthetic albitic

192   glass (EtC, Bureau et al. 2001) and a San Carlos olivine. The resulting precision on the chemical

193   analysis was approximately 1 wt.%.

194 Transmission Electron Microscopy (TEM) investigations were performed at UMET, Lille

195 (France) using a FEI Tecnai G2-20 twin operating at 200 kV.

196 **3. Results**

197

198   Details of the experiments are presented in Table 2. Graphite, which was added in

199 excess, remained as large black globules. The solid powdered run products were composed of

200 diamond seeds embedded in a silicate matrix. For all samples we observed glasses either

201 associated with the crystalline matrix (large glassy areas more or less vesiculated, Figure 1B)

202 or embedded within the new diamond grown around the seeds (Figure 1D). The fact that the

203 glass is massive and does not show quench textures is indicative of equilibrium between the

204 two fluids coexisting at high pressure and high temperature: a carbonate-rich silicate melt

205 (quenched as a glass) and an aqueous fluid (lost on opening), and shows that the melt was fluid

206 saturated.

207   The mineralogical assemblages present in the solid matrix differ depending on the

208 sample set, as described in Table 2.

209   Set 1 corresponds to samples #H3908, #H3911, #H3912 (Figure 2). Diamond growth

210 on seeds is observed for these 3 samples. The concentration of chlorine in the solution (10 g/l

211 for #H3908, 1400°C, 30 g/l for #H3911 at 1400°C and #H3912 at 1300°C) appears to affect

212 diamond growth. Diamond growth is greater for #H3908 (Figure 2A, 10 g/l NaCl, 6 hours),

213 than for #H3912 (Figure 2C) and #3911 (30 g/l NaCl, 6 and 30 hours respectively). Samples

214 #H3908 and #H3911 are comparable because they were run at the same pressure, temperature

215 and duration conditions but with different salinities. From these two experiments it is possible

216 that the high salinity lowers the rate of diamond growth. Diamonds seeds are covered by small

217 round crystals of carbonates and new octahedral diamonds form on the seed surface in the

218   preformed inclusion sites (Figure 2D). Samples #H3911 and #H3912, are comparable in

219   pressure and salinity but were performed at 1400°C and 1300°C for 6 and 30 hours respectively.

220   Based on SEM images, we observe less growth on seeds in sample #H3912 than sample

221   #H3911, demonstrating that temperature is one of the main factors controlling diamond growth.

222   Set 2 corresponds to samples #S5970, #H3913 (Figure 3). In these samples there is a

223   significant increase in the proportion of diamond overgrowth on seeds, a factor of 10 was

224   measured by SEM in the run #S5970 (30 g/l NaCl, 30 hours, figure 3A) compared to the run

225   #H3913 (same conditions, 6 hours, figure 3B). The presence of iron (siderite) affects the

226   mineralogical assemblage of the silicate matrix, which is composed of silicates and carbonates.

227   For sample #S5970 only, we observe small KCl crystals (Figure 3C) probably precipitated from

228   the fluid during the quench. Spontaneously nucleated octahedral diamonds are observed in the

229   solid matrix (Figure 3D).

230   Set 3 corresponds to sample #H3915 (Figure 1D). This experiment is chlorine free, and

231   diamond growth is observed on all of the seeds. The matrix is composed of olivine, CaMg-

232   carbonates and alumina spinel and vesiculated glass (Figure 1B). This implies that the presence

233   of Cl does not affect the mineralogical assemblage present, when compared to similar

234   experiments performed with pure water.

235   Set 4 corresponds to samples #209, #210, #211. For this specific series, runs were

236   performed with a natural basalt and a natural pelagic sediment (Ca-carbonate dominant).

237   Diamond growth was observed only in one experiment, sample #210, which was performed at

238   7 GPa, and 1350°C. For #210 graphite was present, whereas no graphite was added for the run

239   #209. For the experiment #211, performed at lower pressure, 6 GPa, and at 1400°C, a loss of

240   fluid was noticed during the run explaining the absence of diamond growth. In sample #210,

241   spontaneous nucleation of diamond occurred in the matrix (Figure 3). Diamond seeds exhibit

242   trigon features (Figure 4). These etched features might have been formed when the seeds were

243 heated in the air at 1000°C in a furnace before the run. Trigons may also be due to diamond

244 dissolution in a fluid but this is in contradiction with the presence of new diamond crystals in

245 the matrix (spontaneous growth). We attribute the trigons to a growing process on seeds during

246 the short time scale of the experiment (6 hours). The silicate matrix is composed of MgO-rich

247 glasses, containing Na and Cl (Figure 1C), and Ca-Na carbonates. The experiment in the

248 presence of a fluid phase exhibits very little diamond growth, possibly because very little

249 calcium carbonates is dissolved in the fluid at 1350-1400°C and 6-7 GPa. This would mean

250 that graphite (still present as a globule in the solid product) does not participate in the diamond

251 growth.

252 Minerals and glasses from experimental sets 1 to 4 have been analyzed by SEM

253 combined with an EDX analyser, as many of the phases are too small to be investigated with

254 an electron microprobe. The analyses all contain a strong carbon signal due to the use of carbon

255 tape for the sample seat and/or due to the presence of the diamond seeds (Table 3). While a

256 glass phase is always present, we observe different mineralogical assemblages depending on

257 the composition of the starting materials. Set 1: minerals present in the matrix are phengite,

258 rutile, Ca,Mg carbonates and coesite. No chlorine is found in the compositions, suggesting that

259 it remained dissolved in aqueous fluids. Set 2: these runs have been performed in the presence

260 of natural siderite, however iron was not detected in the solid phases. In previous experiments

261 it has been shown that siderite can be dissolved in aqueous fluids at high pressure and

262 temperature (Marocchi et al., 2011). Most of the iron may have been either dissolved in the

263 fluid phase, or possibly alloyed with the Pt capsule during the run, as the latter were not Fe-

264 saturated prior to the experiment. Phengite is not observed but olivine, Ca,Mg carbonates,

265 spinel, and small KCl minerals are deposited on the surface of the diamond seeds (that we

266 attribute to precipitation from the fluid at room conditions). Set 3: this experiment performed

267 in the presence of pure water instead of saline fluids exhibits the same mineralogy to that of set

268   2 (except that KCl precipitates are absent) suggesting that the presence of chlorine does not

269   affect the mineral assemblage. Set 4: experiments have been performed using natural powders

270   of MORB (basalt, Table 1) and pelagic sediments ($CaCO_3$ – SiO_2, Table 1). For this set of

271   experiments the starting materials were crystalline but the final products are mostly glassy

272   suggesting that the conditions of the experiments #209 and #210 were above the solidus.

273   The presence of chlorine in the system does not affect the mineral assemblages, but it

274   does affect the kinetics of diamond growth. Indeed we observe that when Cl is present in large

275   amounts (30 g/l NaCl, #S3911), we observe less diamond growth than for runs performed with

276   lower concentrations of Cl (10 g/l NaCl, e.g. #H3908). Two experiments were run for durations

277   of 30 hours (#S5970, #H3912), allowing significant diamond growth on seeds despite a high

278   salinity. In experiments performed at 1400-1600°C, 7 GPa, in MgO-SiO_2-H_2O-C-KCl or -NaCl

279   system (water being added as brucite), Fagan and Luth (2010) suggest that NaCl may inhibit

280   diamond growth, whereas KCl favors it. Therefore, a competition would be expected during

281   experiments between water and NaCl, the former favoring growth while the latter inhibits

282   diamond growth. In comparison to Fagan and Luth (2010), our experiments were carried with

283   an excess of fluid water that may have resulted in the overall promotion of diamond growth.

284   Inclusions are systematically trapped by diamond during diamond growth in

285   experimental sets 1, 2 and 3. The initiation of inclusion formation is observed at the growing

286   surface of diamonds (see Figure 2D). FIB preparation was performed on a selection of

287   diamonds from experimental sets of samples 1 and 2. The diamonds were sliced open on one

288   face and ion beam polished in order to allow trapped inclusions to be observed. Then the

289   diamonds were sliced on the other face in order to obtain 2-5 µm thick sections. The sections

290   are deposited on silicon wafers with the FIB micromanipulator for SEM investigation. The

291   inclusions can be either located along planes, corresponding to the original surface of the

292   oxidized diamond seeds or isolated within the new diamond areas. Inclusions may be (1)

293 monocrystalline, with different inclusions of different mineralogy appearing close to each other,

294 (2) multi-phased, having trapped different minerals in one cavity together with voids of

295 irregular shape, originally filled with fluid or (3) pure fluid (see Figure 5B). Thus a number of

296 different mineral phases may be associated together, with the same mineralogy as the solid

297 matrix surrounding the diamonds.

298 In sample #3908 (set 1, Figure 5), inclusions are diamonds, Ca-carbonates, phengites,

299 coesites and rutiles. They have been trapped on a plane, probably corresponding to the original

300 surface of the oxidized diamond seed. The presence of empty non-geometrical isolated cavities

301 in diamonds (voids) shows that aqueous fluid inclusions were trapped as a single fluid at the

302 same time as the mineral phases in the diamonds during their growth (e.g. Figure 5). The

303 presence of a silicate glass in the solid matrix shows that a silicate melt was also present.

304 Therefore the diamonds were growing in the presence of two distinct immiscible fluids, a

305 silicate-carbonate melt (quenched as a glass) and a brine (aqueous salty fluid). We found no

306 evidence for the presence of another fluid phase (molten salt or carbonatitic melt). The

307 compositions of the inclusions obtained using EDX are presented in Table 4. The brines were

308 lost as the inclusions were opened using the gallium beam.

309 For samples from set 2, the mineral inclusions trapped in the diamonds also exhibit the

310 same mineralogy as the matrix, together with void spaces. The 2µm thick sections obtained

311 from diamonds from sample #S5970 revealed isolated olivine inclusions and Ca-rich carbonate

312 inclusions (Table 4, uncontaminated analysis). A thin section of 90 nm was prepared for TEM

313 investigation with the FIB for sample #S5970 (Figure 6). TEM investigation of the thin section

314 shows evidence for a new growth area limited by grain boundaries, likely remnants of the initial

315 surface of the diamond seeds. This is similar to diamond growth observed in Bureau et al.

316 (2012). For this long duration and high salinity experiment (30 hours, 30 g/l NaCl, 1300°C),

317 the extent of the growth was not as great as for sample #H3908 (6 hours, 10 g/l NaCl, 1400°C),

318 and corresponds to only a few µm of monocristalline diamond rims, while diamond growth was

319 of more than 10 µm for sample #H3908.

320   Diamond growth rate is very difficult to measure because the growth is not isomorphic.

321 This implies that to measure the extent of the growth, diamond should be sliced perpendicular

322 to the direction of the growth with the FIB. The limit between the original seeds and the new

323 diamond areas are also difficult to define without transmission microscopy investigation. In the

324 case of the sample #S5970 (Figure 6), which was sliced perpendicularly to a new face, grain

325 boundaries can be observed through investigation with the TEM that show the growth to be of

326 about 2 µm after 30 hours at 1300°C, 7 GPa. This is confirmed by the distance between

327 inclusions and rims observed in other FIB sections performed for the same sample. This

328 corresponds to a maximum rate of 0.07 µm/h (or 584 µm/year).

329   For sample #H3908 (1400°C, 7 GPa, 6 hours), the growth was the greatest and therefore

330 the fastest. The extent of growth can only be estimated from SEM photographs because the

331 diamond was excavated with FIB parallel to the growth direction in order to expose the

332 inclusions. Approximately 10 µm of growth is estimated, which would correspond to about

333 1.67 µm/h (or 14 mm/year). This last value is higher than previous rates of crystallization for

334 diamond measured at 0.1–0.3 µm/h in hydrous kimberlite melts (up to 8 wt.% of H_2O) at 7.5

335 GPa, 1400-1450°C (Palyanov et al., 2015) confirming that excess water favors diamond

336 growth.

337   To conclude, for the experimental sets 1 and 2 that have been investigated by FIB, the

338 phases present in the matrix (mineral and fluid phases) coexisting with the diamonds are also

339 trapped as multi-phase inclusions within the newly formed diamond. In the case of the

340 experiments performed with starting materials close to natural rock compositions (set 2), the

341 mineralogical assemblages trapped as inclusions are similar to mineralogical assemblages

342 found in natural diamonds from the upper mantle, olivine (major mineral phase of peridotitic

343   diamonds, e.g. Harte, 2010) and carbonates (e.g. Schrauder and Navon, 1994). For diamonds

344   of set 3, which were not sectioned using FIB, the solid products exhibit the same mineralogy

345   as set 2 (no effect of Cl on the mineralogy but on kinetics) and the same extent of diamond

346   growth, implying that inclusions were trapped during growth. The observations of (1) very poor

347   diamond growth of sample #210 from the set 4 (basalt, calcite and fluid), (2) that calcite was

348   not dissolved in the fluid at these pressure and temperature conditions, and (3) that graphite is

349   still present in the solid products after the experiments: leads us to conclude that diamonds may

350   grow from the carbonates dissolved in the fluid phases and not directly from graphite.

351

352   **4. Discussion**

353

354   *4.1 Processes for diamond growth in fluids*

355   The diamonds synthetized in this study have grown in two coexisting C-O-H bearing

356   fluids (water or brine + carbonate-rich silicates) at pressures and temperatures relevant to the

357   upper mantle, following a typical mantle geotherm (1400°C, 7 GPa). This is shown by the

358   association of aqueous fluid inclusions and solid silicate inclusions in the synthetic diamonds.

359   Excess water promotes significant diamond growth even at low temperatures (1300°C) and

360   promotes a fast growth process, which is a kinetic prerequisite to the formation of inclusions

361   (Roedder, 1984). Furthemore, the diamonds synthetized during experiments from set 1, 2, and

362   3 mimic quite closely morphologies observed in natural monocrystalline octahedral and

363   polycrystalline diamonds.

364   Carbon was present in all experiments as excess graphite and carbonates. The growing

365   medium was buffered by excess water. In experiments from set 1, 2 and 3, graphite and calcium

366   carbonates are still present as solid minerals at the end of the runs (e.g. Ca,Mg-bearing

367 carbonates Figure 2D), suggesting that only sodium and potassium carbonates have broken-

368 down during the experiments because they were not stable at these pressuresand temperatures

369 or under such fluid saturated conditions. Calcium carbonates would be stable coexisting with

370 fluid/melt at high pressures and temperatures, in agreement with experimental studies

371 performed for dry systems (Shatskiy et al., 2016 and references therein). Alkali carbonates

372 were dissolved in the fluid/melt and have likely participated in diamond growth. Indeed,

373 Pal'Iyanov et al. (1999) have shown that these carbonates are catalyzing diamond growth.

374 Furthermore it has been reported that water-bearing carbonate melts are silicate solvents

375 (Dalton and Presnall, 1998).

376   Diamonds can be demonstrated to be growing in the presence of these two fluids

377 because (1) they trap fluid and silicate inclusions (Figure 5), (2) the two fluids (aqueous and

378 silicate-carbonate-melt) are not miscible at the conditions of the experiment (Bureau et al.,

379 2012); (3) fluid and glass are present at the quench. We cannot determine whether diamonds

380 are growing from the melt or from the fluid at these pressures and temperatures.

381   Bureau et al., (2012) suggested the participation of graphite in diamond precipitation.

382 But, the presence of large graphite globules and very little growth observed in experiments

383 performed at conditions where carbonates are not dissolved in the fluid/melt suggests that

384 graphite may not be directly involved in the diamond formation process. Rather diamond

385 formation requires carbon species dissolved in the oxidized fluids/melts. Because aqueous

386 fluids and silicate carbonate-rich melts are both present during the growth (Bureau et al., 2012),

387 an important issue is to determine if diamonds are growing from carbon species in the melt or

388 in the aqueous fluid. At these conditions, in silicate melts carbon must be dissolved as carbonate

389 anions CO_3^{2-} (principally combined with Na, K) or molecular CO_2 (see Holloway and Blank,

390 1994). Thermodynamic calculations argue that carbon speciation in C-O-H super critical

391 aqueous fluids involves $CO_{2,aq}$ and $CH_{4,aq}$ species with the possible involvement of organic

392 anions, such as $CH_3CH_2COO^-$, $HCOO^-$, HCO_3^-,, particualry at low temperatures (Sverjensky

393 et al., 2014). Organic C-O-H species have been observed in diamond-bearing ultrahigh-pressure

394 rocks with a subduction origin (Frezzotti et al., 2011). This is also in agreement with *in situ*

395 siderite dissolution experiments in aqueous fluids at the conditions of shallow subduction (i.e.

396 siderite dissolution at 400°C and up to 1.15 GPa, in pure water and saline fluids, Marocchi et

397 al., 2011), where formic acid (HCOOH), and formaldehyde (HCOH) were observed using

398 Raman spectroscopy. At temperatures higher than 850°C and 5 GPa, however, calculations

399 predict that the dominant species would be $CO_{2,aq}$ (similar to silicate melts) and $CH_{4,aq}$

400 (Sverjensky et al., 2014).

401   At the experimental conditions investigated in this study, the dominant species in the

402 aqueous supercritical fluids are likely to be H_2O and $CO_{2,aq}$. Two mechanisms are possible: (1)

403 If diamonds are growing from the carbon dissolved in the melt, CO_3^{2-} is involved, and (2) if

404 diamonds are growing from the aqueous fluids, $CO_{2,aq}$ is involved.

405 Then the following reactions are proposed, involving constituents from both fluids:

406 Set 1:

407       $12\ Al_2O_3 + 4\ MgO + 2\ K_2CO_3 + 16\ SiO_2 + 4\ H_2O_{\text{aq or melt}} + 2\ CO_{2\ \text{aq or melt}}$

408 $=$

409       $4\ K(AlMg)_2(OH)_2(SiAl)_4O_{10\ \text{phengite}} + 4\ C_{\text{Diamond}} + 19\ O_2$

410   (1)

411 Set 2:

412       $3\ Al_2O_3 + 3\ MgO + 2\ (Fe,Mg)CO_3 + 3\ SiO_2 + 2\ K_2CO_3 + 2\ Na_2CO_3 + 3\ CaCO_3$

413                          $+ 2\ H_2O_{\text{aq or melt}} + 2\ CO_{2\ \text{aq or melt}}$

414

415 $=$

416         $(Fe,Mg)_2SiO_4$ olivine $+$ $MgAl_2O_4$ spinel $+$ 10 $C_{Diamond}$ $+$ 12 O_2 $+$ $(Ca,Mg)CO_3$

417         $+$ 2 $(Na, K)_2(Ca, Mg)Al_2SiO_7H_2O$ "Glass"
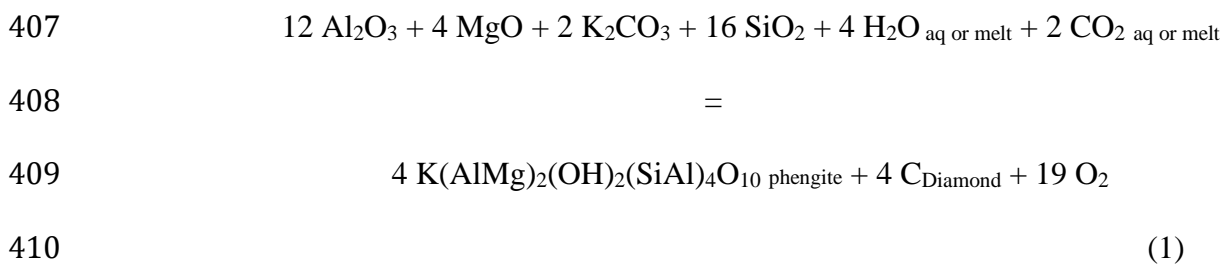
418   (2)
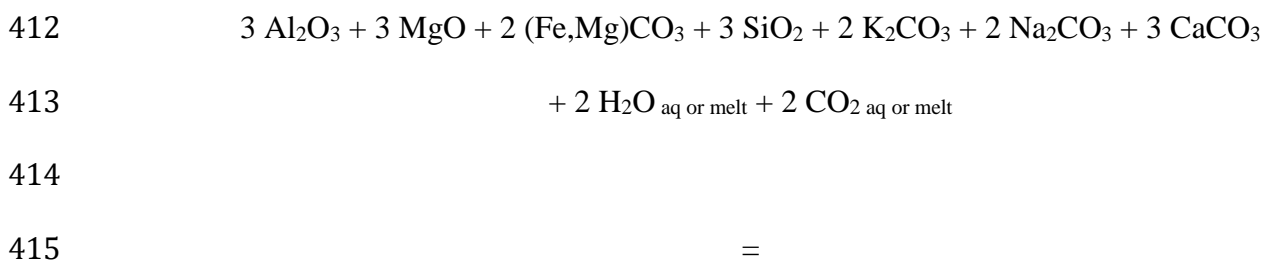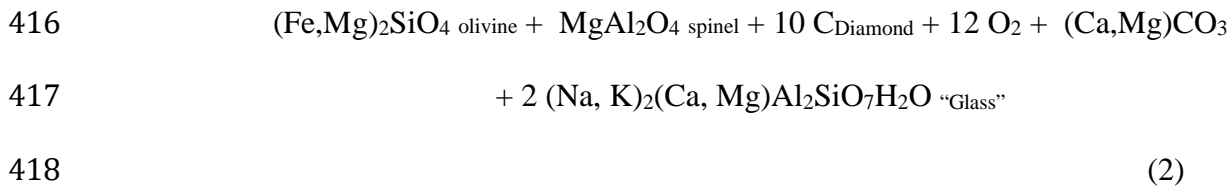
419   In both cases diamond formation would result in oxidation of the surrounding medium,

420 in agreement with the idea that diamonds are metasomatic minerals.

421   The experimental results can be extrapolated to conditions below those of the

422 lithosphere, as the temperature effect was investigated up to 1700°C (Bureau et al., 2012) and

423 shows that the higher the temperature, the more diamonds grow from what is then a single

424 supercritical fluid/melt. Investigation of the effects of pressure was made up to 9 GPa in a

425 previous study (Bureau et al., 2012). In the upper mantle for a fertile peridotite at a temperature

426 of 1200°C, pressure > 6-7 GPa, and relevant fO$_2$, predicted C-O-H fluid speciation along the

427 upper mantle adiabat suggests that H_2O and CH_4 are the major C-H species in C-O-H fluids

428 (Frost and McCammon, 2008). This is corroborated by Raman characterization of coexisting

429 aqueous fluids and melts at pressures and temperatures relevant to the upper mantle that reveal

430 the presence of CH_3 or CH_4 species, (Mysen and Yamashita, 2010; Mysen, 2013). Diamonds

431 cannot grow from aqueous fluids below the lithosphere. The parent fluid is possibly a water-

432 rich melt (supercritical) that is thermodynamically stable at these depths. It is probably from

433 such a melt that the diamond carrying the recently discovered hydrous ringwoodite inclusion

434 found by Pearson and co-workers (2014) grew.

435   Another recently discussed aspect concerning diamond growth in fluids is the potential

436 impact of pH drop when diamonds are growing in aqueous fluids at low pressure and

437 temperature conditions (900°C, 5 GPa, Sverjensky and Huang, 2015). Indeed such a drop would

438 enhance diamond precipitation during water-eclogitic rock interactions without changes in

439 oxidation state. In our experiment whatever the speciation of volatiles are, diamond can

440 precipitate. For example, assuming that diamond precipitates from the aqueous fluids, and that

441   C-O-H species are stable at 7 GPa, 1300-1400°C, a potential reaction may be expressed

442   involving aqueous species (set 1):

443                $12\ Al_2O_3 + 8\ MgO + 2\ K_2CO_3 + 16\ SiO_2 + 4\ HCOO^-_{\ aq} + 8\ H^+_{\ aq}$

444                            $=$

445                $4\ K(Al,Mg)_2(OH)_2(Si,Al)_4O_{10\ phengite} + 6\ C_{Diamond} + 20\ O_2 + 2\ H_2O$

446   (3)
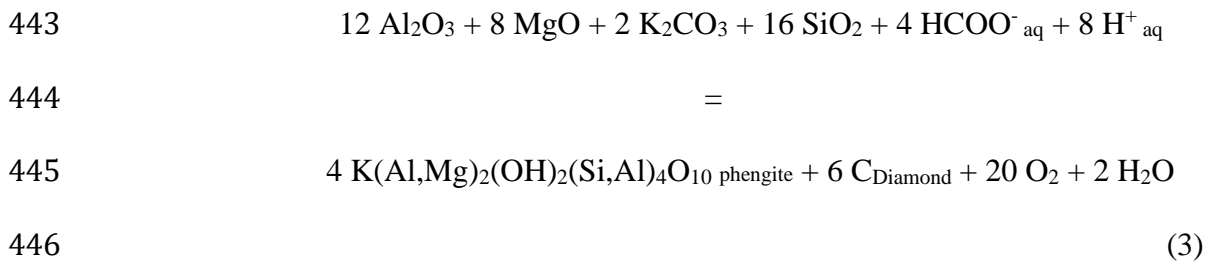
447

448   This equilibrium would be a function of the pH ($-\log[H^+]$) and of the oxygen fugacity

449   (fO_2).

450   In experiments from sets 1 and 2, the species $Na^+_{\ aq}$ and $Cl^-_{\ aq}$ are mutually neutralized

451   (same amounts of HCl and NaOH in the fluid). The pH is determined from the level of

452   interactions between silicates and aqueous fluids. This means that for runs performed at the

453   same pressure, temperature, duration and starting materials, but having15 g/l NaCl or 30 g/l

454   NaCl respectively in the starting solution, the pH should be the same. We observed different

455   diamond growing rates: higher rate of growth for low NaCl content, than for high NaCl content,

456   which cannot be attributed to a pH change.

457   This does not mean that the pH has no effect on diamond growth, but it means that these

458   experiments are not relevant to constrain a potential pH effect on diamond crystallization in

459   aqueous fluids. In the present study, at constant pH, pressure and temperature the extend of

460   diamond growth is affected by the salinity of the aqueous fluid. It implies that a key parameter

461   for diamond growth is the chemical composition of the fluid and its potential effect on the fO_2.

462

463   *4.2 Application to natural cases: comparison with upper mantle natural diamonds*

464

465   About 2 % of natural diamonds gems do contain inclusions (Stachel and Harris, 2008),

466   whether these diamonds are from the upper mantle, the transition zone or the lower mantle (e.g.

467   Shirey et al., 2013 and references therein). Experiments growing inclusion-bearing diamonds

468   are very rare (Bureau et al., 2012). However, comparing inclusions trapped in synthetic

469   diamonds with natural inclusions found in diamond gems is an excellent diagnostic tool to

470   identify the fluids present in the Earth's mantle from which diamonds are growing, and this can

471   be used to describe deep volatiles cycling.

472   Inclusions trapped in diamonds from experimental sets 1 and 2 are syngenetic with the

473   new diamond rims. They reflect the mineralogical composition of the minerals that crystallize

474   on cooling of the fluid/melts: when phengite, coesite, carbonates and rutile are coexisting with

475   the diamonds, they are also trapped as mineral inclusions in the diamond; when olivine, spinel

476   and carbonates are coexisting with the diamonds, they form the mineralogical assemblage of

477   the inclusions in the diamond. This reproduces inclusion assemblages found in natural

478   diamonds.Inclusions from set 2 are similar to the natural inclusions trapped in diamonds from

479   the upper mantle. Indeed we have found olivine, spinel and $(Ca,Mg)CO_3$ trapped as inclusions,

480   i.e. silicate minerals of upper mantle peridotites whereby carbonates are also accessory phases

481   in the mantle. These minerals are commonly found together with fluids, possibly saline, as

482   inclusions in fibrous diamonds (Navon et al., 1988; Schrauder and Navon, 1994; Izraeli et al.

483   2001; Klein Ben David et al. 2009). Diamonds from this study are also comparable with

484   monocrystalline diamonds containing inclusions with a peridotite affinity. Saline fluid

485   inclusions have been described in monocrystalline diamonds (Weiss et al., 2014), possibly

486   having a subduction origin (Weiss et al., 2015). Similarities between fibrous and

487   monocrystalline diamonds have already been pointed out based on trace-element signatures

488   (Rege et al., 2010) and from stable isotope geochemistry (Cartigny et al., 2014 and references

489   therein). These results are relevant to the formation of fibrous coated and cloudy diamonds (e.g.

490   Navon et al., 1988; Schrauder and Navon, 1994; Izraeli et al., 2001; Klein ben David et al.,

491   2007). Because isolated or polycrystalline diamonds spontaneously nucleated in the solid

492   matrix (this study, Bureau et al., 2012), these results are also relevant to diamonds observed as

493   inclusions in minerals from ultrahigh pressure metamorphic rocks of subduction origin that are

494   believed to have grown in subduction zones fluids originating from carbonate dissolution (e.g.

495   Stöckhert et al., 2001; Dobrzhinetskaya, 2012, and references therein; Frezzotti et al., 2014).

496   A recent study (Jablon and Navon, 2016) based on the comparison of fibrous diamond

497   inclusions with micro-inclusions trapped along twinning surfaces of twinned monocrystalline

498   diamonds proposes that all diamonds were grown from high density fluids (HDFs). They

499   suggest that part or most of lithospheric diamonds were formed by carbonate-bearing fluids,

500   similar to those generate during our experiments. We suggest that when they are trapped in

501   diamonds, inclusions are the key to identify the parent fluids. But the rarity of inclusions in

502   monocrystalline diamonds makes this research difficult. Inclusion bearing diamonds must have

503   experienced fast growth events, which may be successive, with one or more batches of

504   metasomatic fluids, each possibly having different compositions. The growth of fibrous coated

505   and cloudy diamonds, containing high density areas of fluid and solid inclusions should be the

506   result of fast and multiple growth events. This was suggested in 1994 by Boyd and coworkers,

507   based on the study of the carbon and nitrogen isotopic composition of coated diamonds. The

508   dynamic nature of diamond growth may cause zonation between silicate and carbonatitic

509   endmembers observed in kimberlite-related diamonds (e.g. Schrauder and Navon, 1994; Klein-

510   BenDavid et al., 2004; 2007; 2010; Van Rythoven et Schulze 2009; Rege et al. 2010). Zonations

511   are also observed in monocrystalline diamonds (e.g. Araujo et al., 2009; Bulanova et al., 2014).

512   This is also compatible with the observation of multiple dissolution events (Klein-BenDavid et

513   al., 2007).

514   The results from this study do not imply that all inclusions trapped in monocrystalline

515   diamonds must be syngenetic. There is natural evidence for protogenetic inclusions trapped in

516   diamonds either based on isotope geochemistry (e.g. Thomassot et al., 2009) or based on

517   inclusion mineralogy (Agrosi et al., 2016). Pre-existing inclusions can be encapsulated in

518   diamonds during their growth in fluids. Assuming that the rarity of inclusions in

519   monocrystalline diamonds may be due to growth kinetic processes, we suggest that this may be

520   related to the amount of water present in the fluid: the more water present, the greater the

521   efficiency that diamonds trap inclusions. Further experiments are necessary to determine if the

522   presence of water may be a key parameter correlating with the proportion of inclusions trapped

523   in diamonds.

524   We confirm the "fluid/melt" origin of diamonds (e.g. Stachel and Harris, 2009), in showing

525   that it is possible to grow diamonds from a range of different complex fluid compositions,

526   providing they contain both carbonates and water. These inclusions will represent their parental

527   fluid/melt, or are the product of interaction between parental fluid/melt and the surrounding

528   mantle. This is in agreement with natural cases, where depending on the depth of diamond

529   growth, we observe inclusions of: peridotitic or eclogitic mineral assemblages for the

530   lithospheric mantle; intermediate mineral assemblages between basaltic and peridotitic

531   compositions in the transition zone (Kiseeva et al., 2013).

532

533   *4.3 Are subduction zones good diamond factories?*

534

535   It is now recognized that at least some natural diamonds grow from subduction zones fluids,

536   originating from oceanic slabs. Eclogitic diamonds form in the deep mantle lithosphere from

537   trapped eclogitic slabs. Some eclogitic and transition zone diamonds exhibit a negative carbon

isotopic signature corresponding to an organic carbon source (see Cartigny et al., 2014 and Shirey et al., 2013 for reviews). A subduction origin for diamonds from the transition zone is also strongly suggested by the discovery of a hydrous ringwoodite inclusion in a diamond from Juina, Brazil (Pearson et. al., 2014). In this last case fluid releases are thought to be generated by the dehydration melting reactions of wadsleyite, ringwoodite, and dense hydrous Mg-silicates formed in slabs (e.g. Ohtani, 2005). Diamonds containing lower mantle mineralogical assemblages, may also grow in deep subduction environments within that same type of protolith because this is the most likely source of oxidized fluids at these depths (Stachel et al., 2005; Harte, 2010). A few studies argue that ultradeep diamonds are growing from subducted oceanic crust "fluids" (Tappert et al., 2005; Walter et al. 2011, Palot et al. 2014). Schmandt and coworkers (2014) interpret the low seismic velocities below the United States of America to the presence of melt in the lower mantle due to the transformation of ringwoodite in bridgmanite in the subducting slabs. The discovery of saline fluid inclusions in monocrystalline diamonds from the Northwest Territories of Canada are attributed to saline fluids from a subducting slab that would be the source for fluid-rich diamonds (Weiss et al., 2015). Other diamonds from South Africa, however, carrying similar saline inclusions (Weiss et al., 2014) display a mantle-like isotopic signature (δ^{13}C centered at -5 ‰) incompatible with a carbon origin either from recycled organic matter or recycled carbonates.

Our experiments suggest that subduction zone fluids are probably the best fluids to grow diamonds because they are possibly enriched in both carbon and water. The high variability of isotopic signatures and the variability of inclusion compositions of natural diamonds probably implies that diamonds are growing in the same manner everywhere in the mantle, i.e. from various carbon-rich fluids including fluids recycled from subduction zones.

5. Conclusion

We show that diamonds can grow at upper mantle conditions in mixtures of silicate melts together with aqueous fluid (possibly saline) and carbonates (dissolved in aqueous fluids or in melts). Depending on the location in the mantle, growth will be associated with silicate melts of different compositions. Depending on the depth of the growth (i. e. pressure and temperature), the process will happen in the presence of aqueous fluid and silicate melt or in the presence of a single supercritical fluid/melt. We show that at upper mantle conditions diamonds are growing from oxidized carbon dissolved either in silicate melts (CO_3^{2-}) or in aqueous fluids (CO_{2aq}), but not from graphite. At a constant pH and oxygen fugacity the extent of growth is dependent on the salinity of the aqueous fluid, suggesting that the key parameter for diamond growth is the chemical composition of the fluid. The speciation of volatile species is not critical providing water is present in excess. This process must be fast in order to promote inclusions trapping during growth. We synthesized diamonds with inclusions (minerals and fluids) trapped in syngenesis with the diamonds. These inclusions reflect the composition of the parent fluids. This shows that, when they are preserved, inclusions and their nature are very good diagnostics to constrain diamond growth conditions in the Earth's mantle. This implies that supercritical fluids/melts are present in the upper mantle and possibly at greater depth, where diamonds grow. This also emphasizes the importance of the deep cycling of major (H, C) and minor (halogens) elements in the mantle and their relevance for natural diamond growth processes.

607

608   **Bibliography**

609   Agrosi G., Nestola, F., Tempesta, G., Bruno, M., Scandale, E., Harris, J., 2016. X-ray

610   topographic study of a diamond from Udachnaya : Implications for the genetic nature of

611   inclusions. Lithos, 248-251, 153-159.

612

613   Araujo, D.P., Griffin, W.L., O'Reilly, S.Y., 2009. Mantle melts, metasomatism and diamond

614   formation: Insights from melt inclusions in xenoliths from Diavik, Slave craton. Lithos, 112S,

615   675-682.

616   Arima, M., Nakayama, K., Akaishi, M., Yamaoka, S., Kanda, H., 1993. Crystallization of

617   diamond from a silicate melt of kimberlite composition in high-pressure and high-temperature

618   experiments. Geology, 21, 968-970.

619   Arima, M., Kozai, Y., Akaishi, M., 2010. Diamond nucleation and growth by reduction of

620   carbonate melts under high-pressure and high-temperature conditions. Geology, 30, 8, 691-694.

621   Boyd, S.R., Pineau, F., Javoy, M., 1994. Modelling the growth of natural diamonds, Chem.

622   Geol 116, 29-42.

623   Bulanova, G.P., Wiggers de Vries, D.F., Pearson, D.G., Beard, A., Mikhail, S., Smelov, A.P.,

624   Davies, G.R., 2014. An eclogitic diamond from Mir pipe (Yakutia), recording two growth

625   events from different isotopic sources. Chemical Geology, 381, 40-54.

626   Bureau, H., Pineau, F., Métrich, N., Semet, M., Javoy, M. (1998). A melt and fluid inclusion

627   study of the gas phase at Piton de la Fournaise volcano (Réunion Island) – Chem. Geol., 147,

628   115-130.

629   Bureau, H., Keppler, H., Métrich, N. (2000) Volcanic degassing of bromine and iodine :

630   experimental fluid/melt partitioning data and applications to stratospheric chemistry, Earth and

631   Planet. Sci. Let., 183, 51-60.

632   Burgess, R., Layzelle E., Turner G., Harris, J.W., 2002. Constrains on the age and halogen

633   composition of mantle fluids in Siberian coated diamonds. Earth and Planet., Sci., Let., 197,

634   193-203.

635   Bureau, H., Langenhorst, F., Auzende, A.-L., Frost, D.J., Estève, I., Siebert, J., 2012. The

636   growth of fibrous, cloudy and polycrystalline diamonds, Geochimica et Cosmochimica Acta,

637   77, 202-214.

638   Cartigny, P., Palot, M., Thomassot, E., Harris, J.W., 2014. Diamond formation: A stable isotope

639   perspective. Annual reviews in Earth and Planetary sciences, 42, 699-732.

640

641   Dalton, J.A., Presnall, D.C., 1998). The continuum of primary carbonatitic-kimberlitic melt

642   compositions in equilibrium with lherzolite: data from the system $CaO-MgO-Al_2O_3-SiO_2-CO_2$

643   at 6 GPa. J. Petrol. 39, 1953-1964.

644

645   De Corte, K., Taylor, W.R., De Paepe, P., 2002. Inclusion contents of microdiamonds from

646   UHP metamorphic rocks of the Kokchetav massif, in: C.D. Parkinson, I. Katayma, J.G. Liou,

647   S. Maryama (Eds.), The Diamond-Bearing Kokchetav Massif, Universal Academy Press, Inc.,

648   Kazakhstan, pp. 115–135.

649

650   Dobrzhinetskaya, L.F., 2012. Microdiamonds – Frontier of ultrahigh-pressure metamorphism:

651   A review. Gondwana research 21, 207-223.

652

653   Fagan, A.J., Luth, R.W., 2010. Growth of diamond in hydrous silicate melts. *Contrib. Mineral.*

654   *Petrol.*, doi 10.1007/s00410-010-0528-9.

655   Frezzotti, M.L., Huizenga, J.M., Compagnoni, R., Selverstone, J., 2014. Diamond formation by

656   carbon saturation in C-H-O fluids during cold subduction of oceanic lithosphere. Geochimica

657   et Cosmochimica Acta, 143, 68-86.

658   Frost, D.J., McCammon, C.A., 2008. The redox state of Earth's mantle, Annu. Rev. Earth

659   Planet. Sci. 36, 389-420.

660   Haggerty, S.E. 1999. A diamond trilogy: superplumes, supercontinents and supernovae Science

661   285, 851-860.

662   Harte, B., 2010. Diamond formation in the deep mantle: the record of mineral inclusions and

663   their distribution in relation to mantle dehydration zones. Mineralogical Magazine, 74(2), 189-

664   215.

665   Holloway, J.R., Blank, J.G., 1994. Application of experimental results to C-O-H species in

666   natural melts, in Volatiles in Magmas, Rev. in Mineralogy, 30, 187-230.

667   Izraeli, E.S., Harris, J.W., Navon, O., 2001. Brine inclusions in diamonds: a new upper mantle

668   fluid, Earth and Planet., Sci., Let., 187, 323-332.

669   Jablon, B.M., Navon, O. (2016) Most diamonds were created equal. Earth and Planet. Sci. Let.

670   443, 41-47.

671   Johnson, L.H., Burgess, R., Turner, G., Milledge, H.J., Harris, J.W., 2000. Noble gas and

672   halogen geochemistry of mantle fluids: comparison of African and Canadian diamonds.

673   Geochimica et Cosmochimica Acta 64, 717-732.

674   Kiseeva, E. S., Yaxley, G. M., Stepanov, A. S., Tkalčić, H., Litasov, K. D., Kamenetsky, V. S.

675   (2013). Metapyroxenite in the mantle transition zone revealed from majorite inclusions in

676   diamonds. Geology, 41, 883-886.

677 Klein BenDavid, O., Izraeli, E.S., Hauri, E., Navon, O., 2004. Mantle fluid evolution – a tale

678 of one diamond. Lithos, **77**, 243-253.

679 Klein BenDavid, O., Izraeli, E.S., Hauri, E., Navon, O., 2007. Fluid inclusions in diamonds

680 from the Diavik mine, Canada and the evolution of diamond-forming fluids. Geochimica et

681 Cosmochimica Acta 71, 723-744.

682 Klein BenDavid, O., Lovinova, A.M., Schrauder, M., Spetius, Z.V., Weiss, Y., Hauri, E.H.,

683 Kaminsky, F.V., Sobolev, N., Navon, O., 2009. High-Mg carbonatitic microinclusions in some

684 Yakutian diamonds – a new type of diamond-forming fluids. *Lithos*, 112S, 648-659.

685 Klein BenDavid, O., Pearson, D.G., Nowell, G.M., Ottley, C., McNeill, J. C.R., Cartigny, P.,

686 2010. Mixed fluid sources involved in diamond growth constrained by Sr-Nd-Pb-C-N- isotopes

687 and trace elements. Earth and Planet. Sci. Let. 289, 123-133.

688 Kurat, G., Dobosi, G., 2000. Garnet and diopside-bearing diamondites (Framesites),

689 Mineralogy and Petrology 69, 143-159.

690 Marocchi, M., Bureau, H., Fiquet, G., Guyot, F., 2011. In-situ monitoring of the formation of

691 carbon compounds during the dissolution of iron (II) carbonate (siderite). Chem. Geol. 290,

692 145-155.

693

694 Metrich, N., Rutherford, M.J. (1992) Experimental study of chlorine behavior in hydrous silicic

695 melts. Geochimica et Cosmochimica Acta 56, 607-616.

696

697

698 Mikhail, S.,Dobosi, G., Verchovsky, A.B., Kurat, G., Jones, A.P. (2013) Peridotitic and

699 websteritic diamondites provide new information regarding mantle melting and metasomatism

700 induced through the subduction of crustal volatiles. Geochim. et Cosmochim. Acta, 107, 1-11.

701

702 Mikhail, S., Verchovsky, A.B., Howell, D., Hutchinson, M.T., Southworth, R., Thomson, A.R.,

703 P., Warburton, Jones, A.P., Milledge, H.J., 2014. Constraining the internal variability of the

704 stable isotopes of carbon and nitrogen within mantle diamonds. Chemical Geology 366, 14-23.

705

706 Mysen, B.O., Yamashita, S., 2010. Speciation of reduced C-O-H volatiles in coexisting fluids

707 and silicate melts determined in situ to 1.4 GPa and 800°C. Geochimica et Cosmochimica Acta

708 74, 4577-4588.

709

710 Mysen, B.O., 2013. Structure-property relationships of COHN-saturated silicate melt

711 coexisting with COHN fluid: a review of in situ, high temperature, high-pressure experiments.

712 Chemical Geology 346, 113-124.

713

714 Navon, O., Hutcheon, I.D., Rossman, G.R., Wasserburg, G.J., 1988. Mantle-derived fluids in

715 diamond micro-inclusions. Nature 335, 784-789.

716 Novella, D., Bolfan-Casanova, N., Nestola, F., Harris, J.W., 2015. H_2O in olivine and garnet

717 inclusions still trapped in diamonds from the Siberian carton: Implications for the water content

718 of cratonic lithosphere peridotites. Lithos 230, 180-183.

719 Ohtani, E., 2005. Water in the mantle, Elements, 1, 25-30.

720

721 Palot, M., Cartigny, P., Viljoen, F., 2009. Diamond origin and genesis: A c and N stable isotope

722 study on diamonds from a single eclogitic xenolith (Kaalvallei, South Africa). Lithos 112S,

723 758-766.

724

725 Pal'yanov, Y.N., Sokol, A.G., Bozdov, Y.M., Khokhryakov, A.F., Sobolev, N.V., 1999.

726 Diamond formation from mantle carbonate fluids, Nature, 400, 417-418.

727 Pal'Yanov, Y.N., Sokol, A.G., Bozdov, Y.M., Tomilenko, A.A., Khokhryakov, Z.F., Sobolev,

728 N.V., 2002. Diamond formation through carbonate-silicate interaction. *Amer. Mineral.*, **87**,

729 1009-1013.

730 Pal'Yanov, Y.N., Sokol, A.G., Tomilenko, A.A., Sobolev, N.V., 2005. Conditions of diamond

731 formation through carbonate-silicate interaction. Eur. J. of Mineral. 17, 207-214.

732 Pal'Yanov, Y.N., Shatsy, V.S., Soblev N., Sokol A.G. (2007) The role of mantle ultrapotassic

733 fluids in diamond formation, Proceedings of the National Academy of Sciences, 104, 9122-

734 9127.

735 Pal'Yanov, Y.N., Sokol, A.G., 2009. The effect of composition of mantle/fluid melts on

736 diamond formation processes. Lithos 112S, 690-700.

737 Pal'Yanov, Y.N., Sokol, A.G., Khokhryakov, A.F., Kruk, A.N., 2015. Conditions of diamond

738 crystallization in kimberlite melt: experimental data. Russian Geology and Geophysics 56, 196-

739 210.

740 Pearson, G., Brenker, F.E., Nestola, F., McNeill, J., Nasdal, L., Hutchison, M.T., Matveev, S.,

741 Mather, K., Silversmit, G., Schmitz, S., Vekemans, B., Vincze, L., 2014. Hydrous mantle

742 transition zone indicated by ringwoodite included within diamond. Nature, 507, 221-224.

743

744 Rege, S., Griffin, W.L., Pearson, N.J., Araujo, D., Zedgenizov, D., O'Reilly, S.Y., 2010. Trace-

745 element pattern of fibrous and monocrystalline diamonds: Insights into mantle fluids. *Lithos*,

746 118, 313-337.

747

748 Roedder, E., 1984. Fluid inclusions, Reviews in Mineralogy 12.

749

750 Safonov, O.G., Perchuk, L.L., Litvin, Y.A., 2007. Melting relations in the chloride-carbonate-

751 silicate systems at high-pressure and the model for formation of alkali diamond-forming liquids

752 in the upper mantle. Earth and planet. Sci. Let. 253, 112-128.

753

754 Sautter, V., Lorand, J.P., Cordier, P., Bondeau, B., Leroux, H., Ferraris, C., Pont, S., 2011.

755 Petrogenesis of mineral micro-inclusions in an uncommon carbonado. Eur. J. Mineral. 23, 721-

756 729.

757

758 Schrauder, M. and Navon, O. 1994. Hydrous and carbonatitic mantle fluids in fibrous diamonds

759 from Jwaneng, Bostwana, Geochim. et Cosmochim. Acta, 58, 761-777.

760

761 Shirey, S.B., Cartigny, P., Frost, D.J., Keshav, S., Nestola, F., Nimis, P., Pearson, G., Sobolev,

762 N., Walter, M.J., 2013. Diamonds and the geology of mantle carbon, in Reviews in Mineralogy,

763 75, 355-421.

764

765 Shatskiy, A., Litasov, K.D., Palyanov, Y.N., Ohtani, E. (2016) Phase relations on the K_2CO_3-

766 $CaCO_3$-$MgCO_3$ join at 6 GPa and 900-1400°C: Implications for incipient melting in carbonated

767 mantle domains. Amer. Mine. 101, 437-447.

768

769 Schmandt, B., S. D., Jacobsen, T. W., Becker, Z. X., Liu, K. G,. Dueker, 2014. Dehydration

770 melting at the top of the lower mantle. Science, 344, 1265-1268.

771

772 Schrauder, M., Navon, O., 1994. Hydrous and carbonatitic mantle fluids in fibrous diamonds

773 from Jwaneng, Bostwana, Geochimica et Cosmochimica Acta 58, 761-771.

774 Sokol, A.G., Tomilenko, A.A., Pal'Yanov, Y.N., Bozdov, Y.M., Pal'Yanova, G.A.,

775 Khokhryakov, A.F., 2000. Fluid regime of diamond crystallization in carbonate-carbon

776 systems. Eur. J. of Mineral. 12, 367-375.

777 Sokol, A.G., Pal'Yanov, Y.N., 2008. Diamond formation in the system MgO-SiO$_2$-H$_2$O-C at

778 7.5 GPa and 1600°C. Contrib. Mineral. Petrol., 155, 33-43.

779 Stachel, T., Brey G.P., Harris, J.W., 2005. Inclusions in sublithospheric diamonds: glimpses of

780 the deep Earth. Elements, 1, 73-78.

781 Stachel, T., Harris, J.W., 2008. The origin of cratonic diamonds – Constraints from mineral

782 inclusions. Ore Geology reviews, 34, 4-32.

783 Stachel, T, Harris, J.W., 2009. Formation of diamonds in the Earth's mantle, J. Phys. Condens.

784 Matter, 21, 364206.

785

786 Stachel, T., Luth, R.W. (2015) Diamond formation – Where, wen and how ? Lithos, 220-223,

787 200-220.

788

789 Stöckhert, B., Duyster, J., Trepmann, C., Massonne, C., 2001. Microdiamond daughter crystals

790 precipitated from supercritical COH + silicate fluids included in garnet, Erzebirge, Germany.

791 Geology, 29, 391-394.

792

793 Sverjensky, D.A., Stagno, V., Huang, F., 2014. Important role for organic carbon in subduction-

794 zone fluids in the deep carbon cycle. Nature Geosciences, DOI:10.1028/NGEO2291.

795

796 Sverjensky, D.A., Huang, F., 2015. Diamond formation due to a pH drop during fluid-rock

797 interactions. Nature Communications, DOI: 10.1038/ncomms9702.

798

799 Tappert, R., Stachel, T., Harris, J.W., Muehlenbachs, K., Ludwig, T., Brey, G.P., 2005.

800 Subducting oceanic crust: the source of deep diamonds. Geology 33 (7), 565-568.

801

802 Thomassot, E., Cartigny, P., Harris, J.W., Lorand, J.P., Rollion-Bard, C., Chaussidon, M.

803 (2009). Metasomatic diamond growth: A multi-isotope study (^{13}C, ^{15}N, ^{33}S, ^{34}S) of sulphide

804 inclusions and their host diamonds from Jwaneng (Botswana). Earth and Planet. Sci. Let., 282,

805 79-90.

806

807 Thomson, A.R., Kohn, S.C., Bulanova, G.P., Smith, C.B., Araujo, D., EIMF, Walter, M.J.

808 (2014) Origin of sub-lithospheric diamonds from the Juina-5 kimberlite (Brazil): constraints

809 from carbon isotopes and inclusion. Contrib. Mineral. Petrol. 168: 1081.

810

811 Tomlinson, E.L., Jones, A.P., Harris, J.W., 2006. Co-existing fluid and silicate inclusions in

812 mantle diamond, Earth and Planet., Sci., Let., 250, 581-595.

813

814 Tomlinson, E.L., Müller, W., EIMF, 2009. A snapshot of mantle metasomatism: Trace element

815 analysis of coexisting fluid (LA-ICP-MS) and silicate (SIMS) inclusions in fibrous diamonds.

816 Earth and Planet., Sci., Let., 279, 362-372.

817 Van Rythoven, A.D., Schulze, D.J., 2009. In-situ analysis of diamonds and their inclusions

818 from the Diavik Mine, Northwest Territorries, Canada: Mapping diamond growth. Lithos 112S,

819 870-879.

820 Walter, M.J., Kohn, S.C., Araujo, D., Bulanova, G.P., Smith, C.B., Gaillou, E., Wang, J., Steele,

821 A., Shirey, S.B. (2011) Deep mantle cycling of oceanic crust: Evidence from diamonds and

822 their mineral inclusions. Science, 334, 6052, 54-57.

823 Weiss, Y., Kessel, R., Griffin, W.L., Kiflawi, I., Klein BenDavid, O., Bell D.R., Harris, J.W.,

824 Navon, O., 2009. A new model for the evolution of diamond-forming fluids: Evidence from

825 microinclusion-bearing diamonds from Kankan, Guinea, Lithos, 112S, 660-674.

826

827 Weiss, Y., Kiflawi, I., Davies, N., Navon, O., 2014. High-density fluids and the growth of

828 monocrystalline diamonds. Geochimica et Cosmochimica Acta 141, 145-159.

829

830 Weiss, Y., McNeill, J., Pearson, G., Nowell, G.M., Ottley, C.J., 2015. Highly saline fluids from

831 a subducting slab as the source for fluid-rich diamonds. Nature 524, 339-344.

832

833 Zedgenizov, D.A., Kagi, H., Shatsky, V.S., Razogin, A.L. (2014. Local variations of carbon

834 isotope composition in diamonds from Sao-Luis (Brazil): Evidence for heterogeneous carbon

835 reservoir in sublithospheric mantle. Chem. Geol. 363, 114-124.

836

837

Figure captions

839

840 **Fig.1:** SEM pictures of A. starting diamond seeds; B. Vesiculated glass (exp #H3915), shows

841 that the fluid phase was present during the whole run. Vesicles are created by water exsolution

842 from the high pressure fluid/melt during the experimental quench (i.e. decompression); C. Glass

843 (exp #210); D. Grown seeds covered by a thin glassy film (exp #H3915).

844 **Fig. 2:** SEM pictures of the solid products from the set of experiments 1: A. exp #H3908,

845 diamond growth on seeds; B. exp #H3911 diamond growth on seeds; C. exp #3912, diamond

846 growth on seeds, in this last case the growth is smaller than for the two previous runs; D. surface

847 of a diamond from exp #H3908. One can observe small new diamonds and carbonate crystals

848 being trapped as inclusions in the growing surface of the diamond seed.

849 **Fig. 3:** SEM pictures of the solid products from the set of experiments 2: A. growth on diamond

850 seeds from exp #S5970, after a long run of 30 hours duration. The growth is spectacular

851 compared to short run times. Trapping of inclusions occurs at the surface of the growing

852 diamond; B. growth on diamond seeds, exp #H3913 (short run: 6 hours); C. small cubic crystals

853 of KCl at the surface of diamond seeds (#S5970); D. spontaneous nucleation of diamond

854 crystals in the matrix, run #S5970.

855

856 **Fig. 4:** SEM pictures of the solid products from the set 4, experiment #210: A. spontaneous

857 nucleation and growth of diamond in the matrix; B. trigons observed at the surface of the

858 diamond seeds attributed to growth on seeds.

859 **Fig. 5:** SEM pictures of one diamond seed from run #H3908. A. The diamond has been opened

860 with FIB and exhibits primary multi-phased inclusions trapped during diamond growth. B. A

861 zoom of the inclusion area together with EDX analysis (see Table 4) shows that these inclusions

862   are of different compositions: Ca-carbonates, coesite, phengite, rutile and diamonds in grey.

863   Empty cavities that lack a geometric shape do likely correspond to lost fluid inclusions. C. SEM

864   picture of the left area, showing small new diamonds, carbonates, coesite and open cavities (i.e.

865   lost fluid); D. SEM picture of the right area, showing phengite, rutile, and open fluid inclusions.

866   **Fig. 6:** Sample #S5970 (7 GPa, 1300°C, 30 hrs). A. Scanning electron microscopy micrograph

867   of one diamond seed having experienced diamond growth before preparation. The double line

868   represents the thin section position that was sliced by focused ion beam B. Thin section of about

869   200 nm thickness for transmission electron microscopy (TEM) study. C. TEM bright field

870   micrograph reconstruction of part of the thin section. This bright field image exhibits several

871   dark contours (wavy lines) originating from diffraction contrast. One can observe new growth

872   areas at the peak of the thin section delimited by grain boundaries. Grain boundaries are also

873   observed within the seed, corresponding to healed fractures as the synthetic diamond seeds have

874   been crushed and pre-oxidized in the air before the experiments. D. Enlargement of the TEM

875   bright field photograph of the peak of the thin section where one can see the grain boundaries

876   corresponding to remnants of the surface of the starting diamond seed. E. High resolution

877   micrograph of one growth area. TEM investigation shows that the new diamond areas are

878   undistinguishable from the initial diamond from a crystallographic point of view (i.e. same

879   crystal orientation).

880

881

882
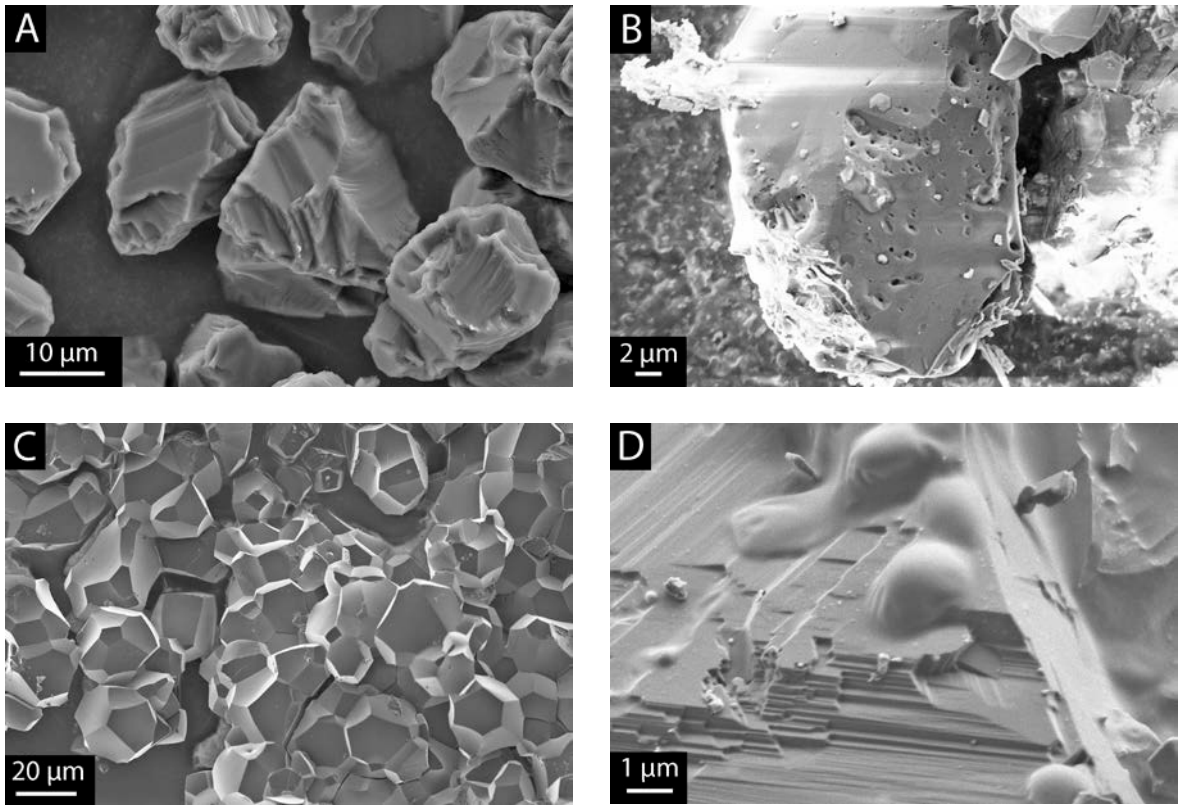
Figure 1

883
884
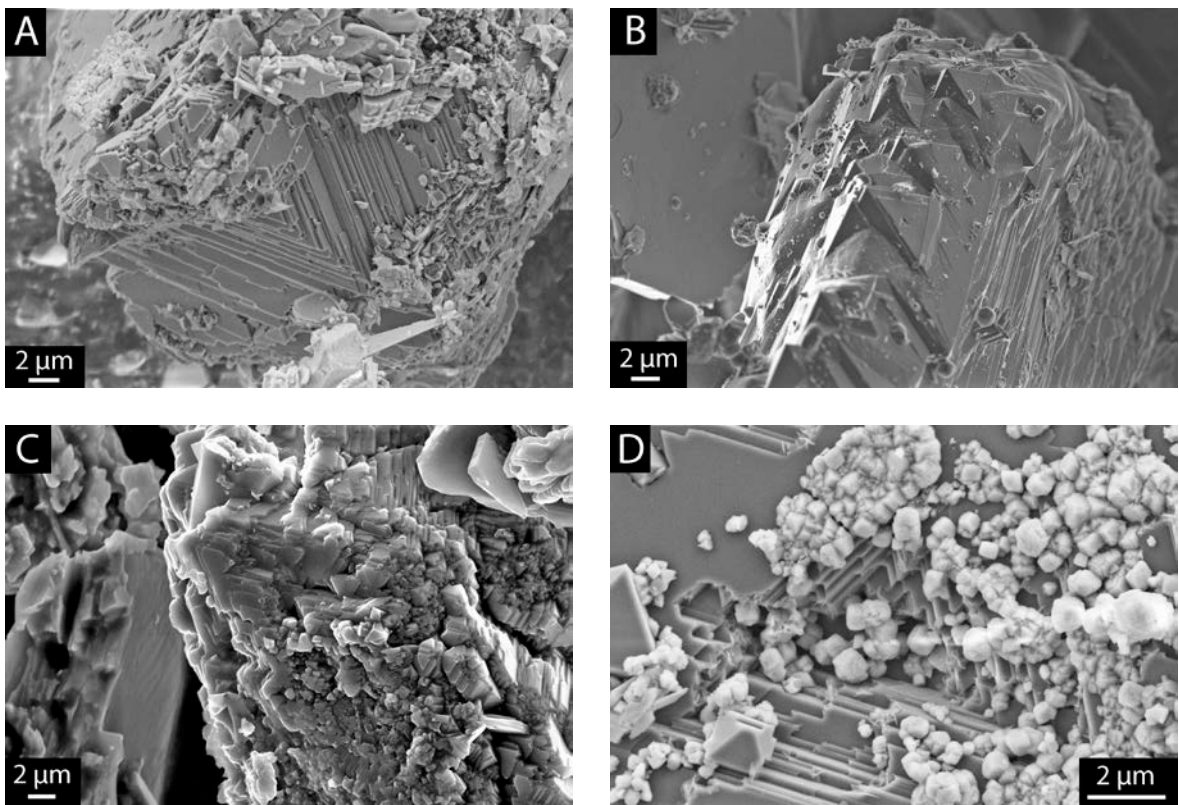
Figure 2

885

886
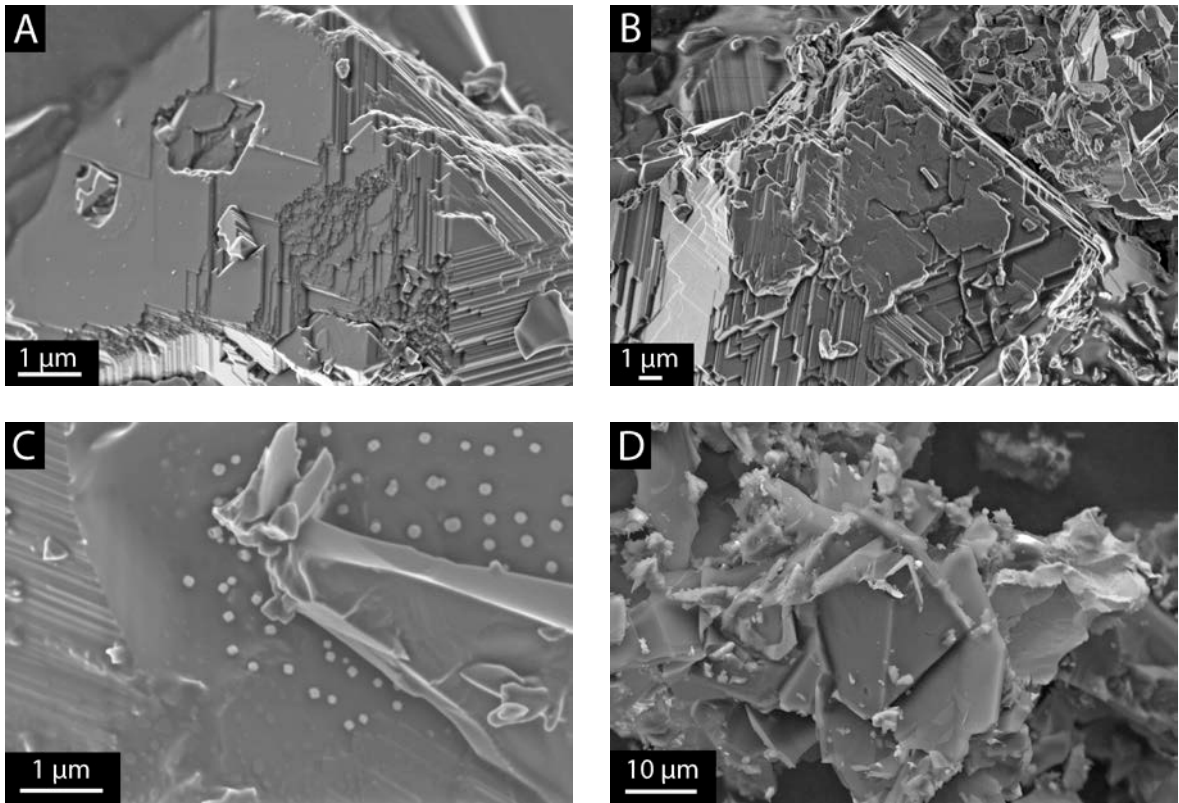
Figure 3

887

888
889
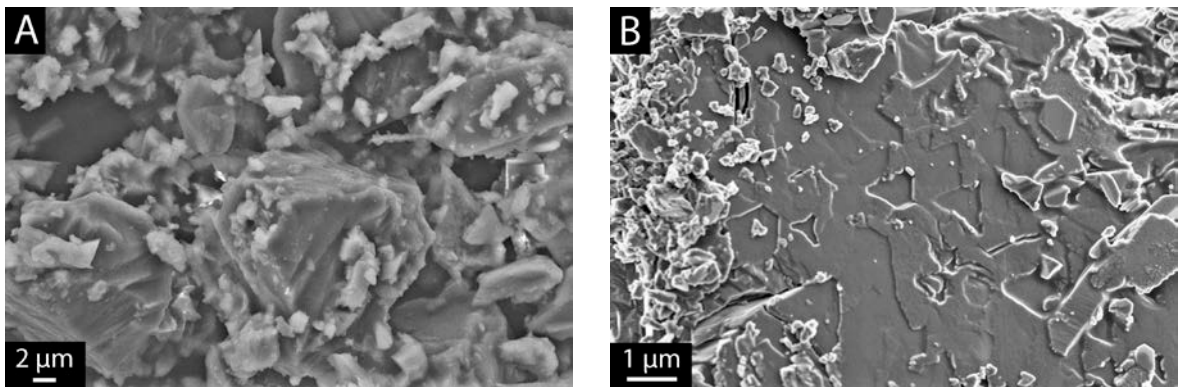
Figure 4

890
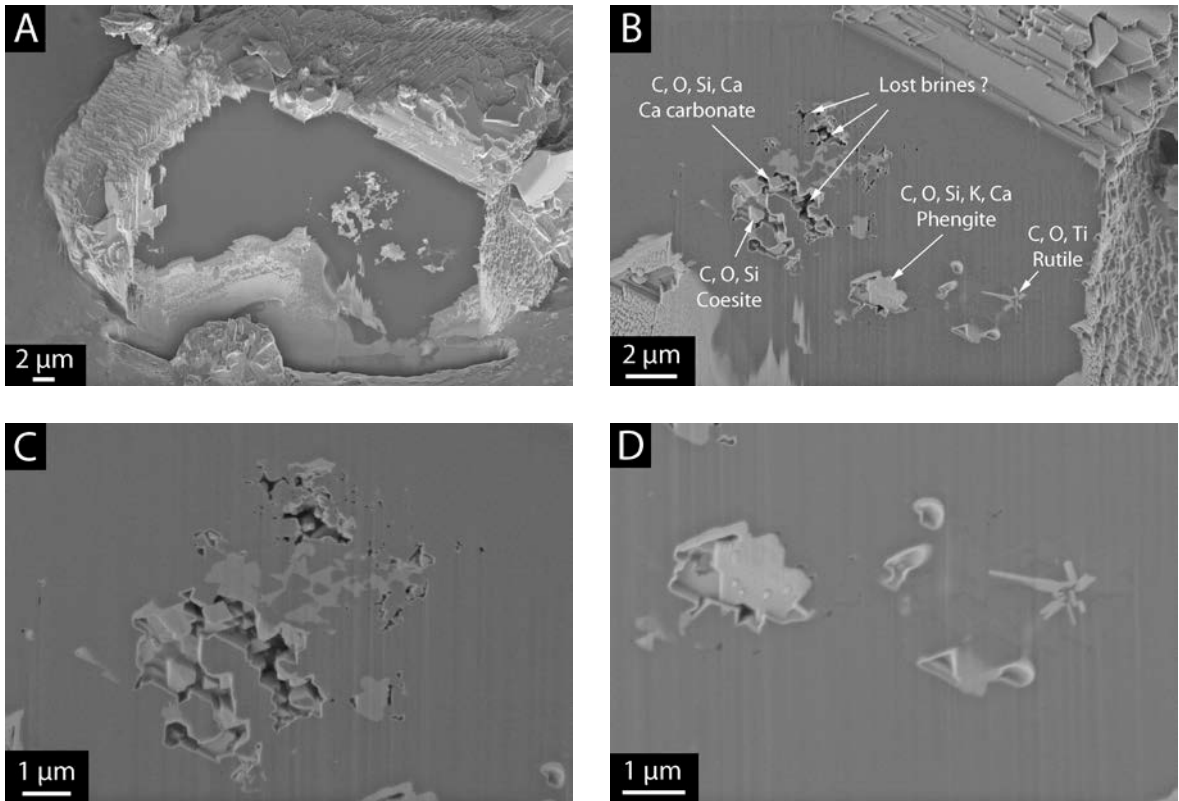
Figure 5
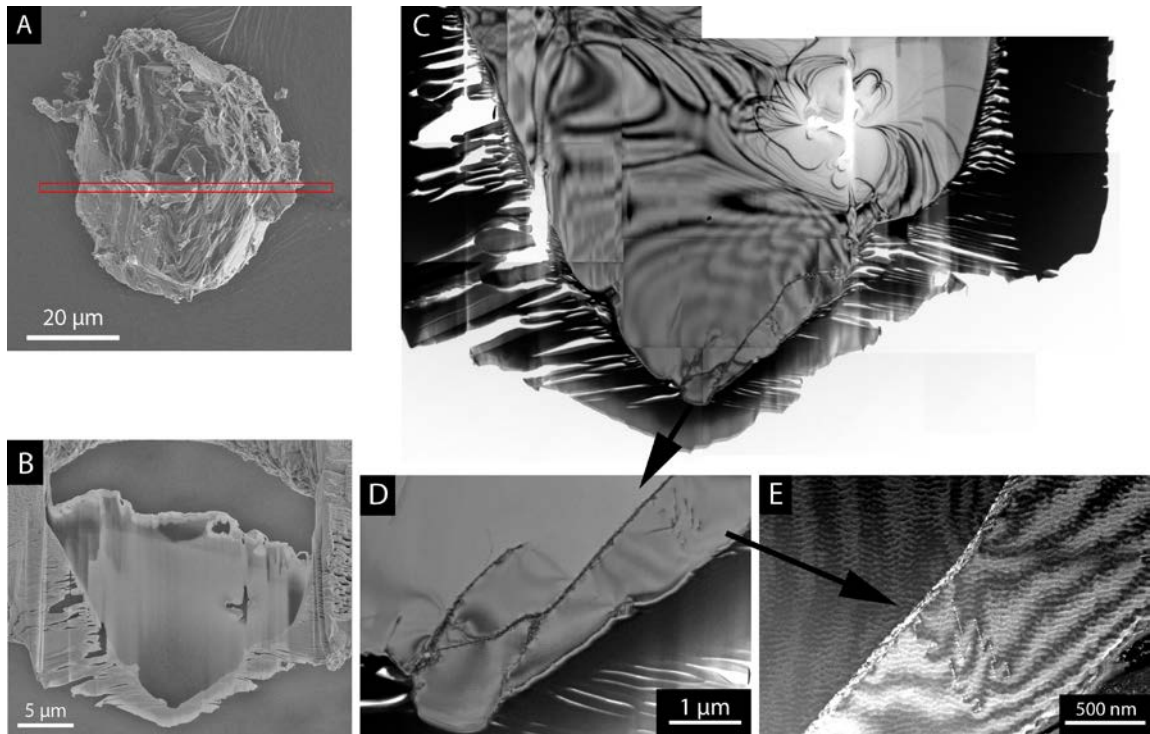
Figure 6

896   **Table 1:** Starting materials

897

Name	Description	Composition
MELD	Mixture of oxides and carbonates[1]	SiO_2 40.47; Al_2O_3 4.36; MgO 21.07; CaO 9.29; Na_2O 2.36; K_2O 17.57; TiO_2 4.89, about 15 wt.% of CO_2
SIDB	Natural siderite[2]	$(Fe,Mg)CO_3$ In at.%: MgO 2.47; FeO 49.11; MnO 7.17; CaO 0.83
SED[3]	Natural pelagic sediment[4] MD85682 Indian ridge	DRX analysis: 97 % $CaCO_3$ + 3% SiO_2
MORB[3]	Natural mid ocean ridge basalt[5] Indian ridge	DRX analysis: 38.26% $CaAl_2Si_2O_8$ 13.25 % $(Mg_{1.41}Fe_{0.59}) SiO_4$ 44.72 % $(Ca_{0.8}Mg_{1.2})Si_2O_6$

898   (1) After Bureau et al., 2012
899   (2) After Boulard et al., 2011
900   (3) DRX analysis after E. Foy
901   (4) From the *Muséum National d'Histoire Naturelle*'s collection.
902   (5) Courtesy of Damien Jaujard
903
904

905

Table 2: Summary of experimental conditions and run products

Name	Starting Materials	P GPa	T °C	Duration Hrs	Results and remarks
#H3908 *Set1*	MELD, H_2O-NaCl 10 g/l, G seedsA	7	1400	6:00	D growth on seeds Matrix: D + phengite + $(Ca,Mg)CO_3$ Coesite + rutile Glass + graphite
#H3911 *Set1*	MELD, H_2O-NaCl 30 g/l, G seedsA	7	1400	6:00	D growth on seeds Matrix: D + phengite + $(Ca,Mg)CO_3$ Coesite + rutile Glass + graphite
#H3912 *Set1*	MELD, H_2O-NaCl 30 g/l, G seedsA	7	1300	30:00	D growth on seeds Matrix: D + phengite + $(Ca,Mg)CO_3$ Coesite + rutile + KCl Glass + graphite
#S5970 *Set2*	MELD+SIDB H_2O-NaCl 30 g/l, G seedsB	7	1300	30:00	D growth on seeds Matrix: D + olivine + $(Ca,Mg)CO_3$ KCl Glass + graphite
#H3913 *Set2*	MELD+SIDB H_2O-NaCl 30 g/l, G seedsB	7	1400	6:00	D growth on seeds Matrix: D + olivine+ $(Ca,Mg)CO_3$ Glass + graphite
#H3915 *Set3*	MELD+SIDB H_2O, G seedsB	7	1400	6:00 +	D growth on seeds Matrix: D + olivine + spinel Glass + graphite
#209 *Set4*	MORB+SED H_2O-NaCl 10 g/l, seedsB	7	1300	6:00	D growth not observed Matrix: D + MgO-rich glass Glass + graphite + $(Ca,Fe,Mg)CO_3$
#210 *Set4*	MORB+SED H_2O-NaCl 10 g/l, G seedsB	7	1350	6:00	Slight D growth on seeds Matrix: D + MgO-rich glass Glass + graphite + $(Ca,Fe,Mg)CO_3$
#211 *Set4*	MORB+SED H_2O-NaCl 10 g/l, G seedsB	6	1400	10:00	Fluid lost No real evidence of D growth on seeds Matrix: MgO-rich glass + $CaCO_3$ Glass + graphite

D diamond, G graphite, seedsA: diamonds 40-60 µm, seedsB diamonds 20-30 µm
Runs #209, #210, #211, AuPd capsules; others Pt capsules

912 **Table 3:** Typical semi-quantitative EDX analysis of the solid phases (matrix) present in the
913 quenched products from samples from the Set1. Analysis were performed for phases large
914 enough (>1µm). Almost all analysis exhibit a strong contamination, measured as CO_2, due to
915 the powders being deposited on carbon tape, and also due to the presence of diamond seeds.
916 Uncertainties are of about 1 wt.%.

	H3908 pheng	H3908 pheng	H3908 pheng	H3908 pheng	H3911 pheng	H3911 pheng	H3912 pheng	H3912 pheng	H3908 rutile	H3908 carb	H3908 carb	H3911 carb
SiO_2	48,4	49,3	52,9	49,2	51,8	50,1	48,6	50,4	8,4	0,0	1,6	1,0
Al_2O_3	5,8	6,0	5,9	6,1	5,9	6,5	4,8	5,8	2,5	0,0	0,5	0,0
Na_2O	0,0	0,0	0,0	0,0	0,0	0,0	0,0	0,0	0,0	0,0	0,7	0,0
MgO	25,5	24,8	22,9	24,5	23,2	24,6	20,8	23,0	2,6	9,0	11,1	0,6
K_2O	18,4	19,9	18,4	19,5	18,2	18,8	24,5	19,6	5,3	0,0	1,1	0,0
CaO	0,0	0,0	0,0	0,0	0,0	0,0	0,0	0,0	2,4	30,3	39,3	55,0
TiO_2	1,9	0,0	0,0	0,8	0,9	0,0	1,3	1,1	78,9	0,0	0,0	0,0
FeO	0,0	0,0	0,0	0,0	0,0	0,0	0,0	0,0	0,0	0,0	0,0	0,0
CO_2	0,0	0,0	0,0	0,0	0,0	0,0	0,0	0,0	0,0	60,7	45,7	43,4
Total	100,0	100,0	100,0	100,0	100,0	100,0	100,0	100,0	100,0	100,0	100,0	100,0

917 pheng phengite, carb carbonate

918

919

920 **Table 3 :** continued, samples from Set2

	S5970 Olivine	S5970 Olivine	S5970 carb	S5970 glass	S5970 glass	H3913 glass	H3913 glass
SiO_2	41,5	47,0	0,0	0,2	0,0	8,4	77,8
Al_2O_3	0,0	0,0	0,0	0,0	0,0	1,7	4,8
Na_2O	0,0	0,0	0,0	0,0	0,0	0,0	0,0
MgO	58,5	53,0	6,3	46,4	100,0	40,3	6,2
K_2O	0,0	0,0	0,0	2,4	0,0	3,8	9,2
CaO	0,0	0,0	0,0	1,7	0,0	36,8	0,9
TiO_2	0,0	0,0	0,0	0,0	0,0	5,3	1,1
FeO	0,0	0,0	0,0	0,0	0,0	0,0	0,0
MnO	0,0	0,0	0,0	0,0	0,0	3,7	0,0
CO_2	0,0	0,0	93,7	49,2	0,0	0,0	0,0
Total	100,0	100,0	100,0	100,0	100,0	100,0	100,0

921

922

923 **Table 3 :** continued samples from Set 3 and 4

Set3	H3915 Olivine	H3915 Olivine	H3915 glass	H3915 spinel	Set4	211 carb	209 glass	210 glass	210 glass	210 glass
						0,0	58,7	33,1	41,3	56,3
SiO_2	42,6	41,5	8,9	0,0		0,0	8,4	9,1	23,5	16,7
Al_2O_3	0,0	0,0	0,3	70,2		0,0	1,6	3,6	1,0	5,9
Na_2O	0,0	0,0	0,4	0,0		5,2	3,3	4,1	12,8	7,5
MgO	57,4	58,5	11,6	29,8		0,0	0,0	0,0	0,0	0,0
K_2O	0,0	0,0	4,6	0,0		32,1	24,0	8,3	17,9	12,5
CaO	0,0	0,0	0,9	0,0		0,0	1,3	0,9	0,0	0,0
TiO_2	0,0	0,0	0,0	0,0		1,8	1,8	0,6	3,5	1,0
FeO	0,0	0,0	0,0	0,0		0,0	0,0	0,0	0,0	0,0
MnO	0,0	0,0	0,0	0,0		60,9	0,0	40,3	0,0	0,0
CO_2	0,0	0,0	73,3	0,0		0,0	0,8		0,0	0,0
Total	100,0	100,0	100,0	100,0		100,0	100,0	100,0	100,0	100,0

924

925

926

927

Table 4: Minerals trapped as inclusions in diamonds, and reference natural basaltic glass
M86 (Bureau et al., 1998). Analysis have been performed on thick sections prepared with
FIB. The analyses are strongly contaminated in carbon from the diamond-hosts, due to the
small size of the inclusions. Uncertainties are of about 1 wt.%.

932

Sample	#H3908 pheng	#H3908 carb	#H3908 rutile	#S5970 Olivine ts	#S5970 carb	M86 glass measured	M86 glass expected
SiO_2	3,0	1,7	0,9	52,9	0,0	47.38	48.65
Al_2O_3	0,0	0,0	0,0	0,5	0,0	14.73	13.93
Na_2O	0,0	0,0	0,0	0,0	0,0	3.51	1.70
MgO	0,0	0,0	0,0	46,6	7,3	8.29	7.48
K_2O	0,3	0,0	0,0	0,0	0,0	0.66	0.62
CaO	0,8	8,6	0,0	0,0	6,6	11.44	11.5
TiO_2	0,0	0,0	18,4	0,0	0,0	2.9	2.83
FeO	0,0	0,0	0,0	0,0	0,0	10.96	10.71
CO_2	96,0	89,7	80,6	0,0	86,0	0,0	0,0
Total	100,0	100,0	100,0	100,0	100,0	100,0	100,0

933

pheng phengite, carb carbonate, ts analysis performed on a thin section for TEM

935